CONF-780508--77

PREPRINT UCRL- 80782

Lawrence Livermore Laboratory

CONCEPTUAL DESIGN CONSIDERATIONS AND NEUTRONICS OF LITHIUM FALL LASER FUSION TARGET CHAMBERS

W. R. Meier and W. B. Thomson

May 31, 1978

This paper was prepared for submission to the Proceedings of the Third ANS Topical Meeting on Fusion, May 9-11, 1978, Santa Fe, New Mexico.

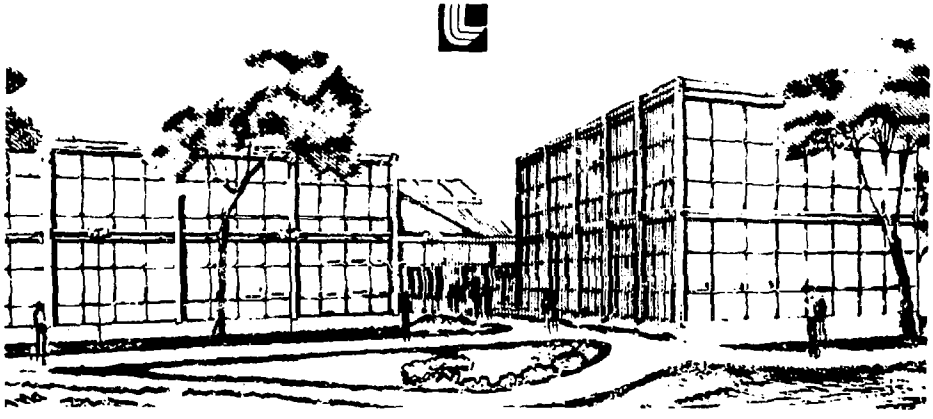

CONCEPTUAL DESIGN CONSIDERATIONS AND NEUTRONICS OF LITHIUM FALL LASER FUSION TARGET CHAMBERS*

W. R. Meier

Lawrence Livermore Laboratory
University of California
Livermore, California 94550

W. B. Thomson

Rockwell International
Atomics International Division
Canoga Park, California 91304

Atomics International and Lawrence Livermore Laboratory are involved in the conceptual design of a laser fusion power plant incorporating the lithium fall target chamber. In this paper we discuss some of the more important design considerations for the target chamber and evaluate its nuclear performance. Sizing and configuration of the fall, hydraulic effects, and mechanical design considerations are addressed. The nuclear aspects examined include tritium breeding, energy deposition, and radiation damage.

TARGET CHAMBER DESIGN CONSIDERATIONS-INTRODUCTION

The following is a brief discussion of some of the more important considerations in the design of a target chamber for a laser fusion central power station. The target chamber is the interface between the laser and power conversion systems and operates in a severe environment. The topics discussed here are in the areas of fall sizing and configuration, hydraulics effects within the chamber, and various mechanical design considerations.

* Work performed under the auspices of the U.S. Department of Energy by Lawrence Livermore Laboratory under contract No. W-7405-Eng-48.

SIZING THE LITHIUM WATERFALL

The lithium waterfall involves a massive flow of lithium on all sides of the microexplosion. To minimize the lithium flow rate, it is desirable to minimize the radial distance to the fall and thus the flow cross sectional area for a given radial thickness. However, if the radial distance to the fall is decreased too much, the x-rays and debris induced vaporization from the inner surface of the fall will generate a high pressure in the small volume available and force the lithium fall into the first wall at a considerable velocity. This effect is discussed in a paper by Hovingh, Blink and Glenn, also presented at this meeting.[1] Therefore, the annular geometry of the fall is a compromise between minimizing the flow rate and minimizing the pressure effects.

In order to provide continuous protection the fall must be reestablished between microexplosions. That is, the fall must drop to a level at or close to the base of the chamber before the next microexplosion occurs. With high yield target (up to 4000 MJ per pulse) the microexplosions need only occur at a rate of roughly one per second to achieve a thermal power sufficient for a GW_e power plant. If a large chamber height is selected (e.g., greater than 10 m), either the repetition rate must be reduced or the nozzle exit velocity at the chamber top must be increased. In the latter case, both the flow rate and the pumping power must be increased. On the other hand a chamber of low height will be subject to greater neutron wall loading and possibly greater pressures from the lithium fall.

SINGLE VS. MULTIPLE FALLS

Fall designs of a wide variety can be envisioned. The simplest is a single annular fall that surrounds the target. The characteristics of even this fall are not entirely understood. For example, it is generally assumed that this fall will thin radially and retain uniform continuity. In fact, care must be taken in the nozzle design to insure that instabilities in the fall in space and time leading to poor first wall protection do not occur.

An interesting modification of the single fall is the double fall. In this case a second, smaller fall is established outside the main fall, starting at a lower height. A double fall has the advantages of reducing the flow rate

and pumping power, and possibly mitigating the impact of lithium on the first wall. Studies have been made of up to five concentric annular falls but there appears to be little advantage in having more than two falls.

JET FALLS

In recent months studies have been made of falls comprised of a large number of closely packed round lithium jets. This concept is discussed in detail in a paper by Maniscalco, et.al., also presented at this meeting.[2] These jets are in the range of 10 to 40 cm in diameter and have a packing fraction up to 50% at the mid-plane. Multiple jet falls have several potential advantages. One is that the separation of the falls will tend to inhibit propagation of shock waves through the lithium. Another advantage is that jet falls will provide a large lithium surface area upon which vaporized lithium may condense, assuming the surface area is sufficiently exposed to the vapor. The open array also prevents the buildup of the internal pressure that can accelerate the annular fall into the wall.

Another possible advantage of jet falls is that the lithium may enter over the entire top of the chamber, thus providing protection which would otherwise be difficult to achieve. A corollary idea in the use of jet falls is that the falls could be parabolic instead of vertically downward. Thus, lithium leaving at the center of the top may be directed outward while that leaving near the outer rim at the top may be directed inward - with the mid-plane fall being at the desired distance from the target. Thus, parabolic jet falls would protect the top of the chamber while forming a more compact fall below. A disadvantage of jet falls is that the lithium is less compact than annular falls which may increase the flow rate for a given effective lithium protective layer, depending on how small the inner radius of the annular fall is allowed to be.

FIRST WALL CONSIDERATIONS

The function of the first wall is to confine the lithium fall from one microexplosion to the next and to withstand the radiation environment (chiefly high energy neutrons) for the life of the plant. The behavior of the lithium flow before and after each microexplosion is discussed in companion papers. It is possible that the fall may impact the first wall with a significant velocity. One way to resist such impact is to use a thick first wall which

provides inertial resistance to impact as well as resistance to sudden internal pressures. A thick first wall has the disadvantage of being vulnerable to thermal stresses generated by the intermittent neutron pulses and lithium flow patterns.

An alternate type of first wall is thinner and porous, allowing a portion of the impacting lithium to pass through the wall. This wall is more flexible but still performs the function of confining the lithium flow to a reasonable extent.

LASER BEAM PORTS

Approximately once a second the laser beams fire at the DT pellet. At this instant the fall should be providing complete protection to the first wall and other structures. However, the laser beams must fire through the fall region without interference, yet without compromising the fall performance. Two ways have been proposed to do this. One is to have tubes inserted through the fall through which the laser beams are fired. This is a positive solution but there are some disadvantages. For one, the penetrations can cause serious disturbances of the flow pattern. In addition, the ends of the tubes are exposed to the ablative action of the microexplosion and will tend to have a short life. Another solution to provide egress for the laser beams is to design the fall to crisscross slightly above the mid-plane, leaving an entrance in the fall for the beams. There is, then, no beam tube to ablate.

INLET NOZZLE DESIGN

The currently preferred inlet nozzle design has a large number of small diameter, convergent nozzles. The lithium head above these nozzles is about one meter. The inlet flow across the top of the nozzle region is essentially at constant velocity so that the turning losses into the individual nozzles is virtually a constant. If the head above the nozzles and the turning loss are both constant, then the nozzle flow will be fairly uniform. However, the nozzle resistances are rather weak; hence, an orifice plate at the upper plane of the nozzles may be needed to effect a more positive control over the nozzle flow.

It would be desirable to have a constant time-rate of flow in the nozzles. However, the impulse that will follow each microexplosion may produce sudden variations in the flow rate in both time and space. The best way to prevent

interruption of nozzle flow is to provide a maximum of protection for the nozzle plate by means of the lithium flow from the nozzles. This implies a large flow area at the nozzle exit which places restrictions on the nozzle inlet/outlet area ratio. Ideally, this ratio should be about 3.0 but a much lower ratio may be required to protect the nozzle. It may be that nozzle flow interruptions are permissible if the flow and, hence, the fall are reestablished satisfactorily.

EXIT NOZZLE DESIGN

At a lithium flow rate of 100 m^3/s and an exit nozzle flow velocity of 6 m/s, the diameter of a single exit nozzle is 4.6 m. Thus, it may be difficult to avoid having a pool at the bottom of the chamber and the consequent shock wave and splash problems. Design of the exit nozzle can be improved by increasing the exit velocity to 12 m/s such that the nozzle diameter is 3.3 m. However, this will be difficult to achieve and will not eliminate the problem. The exit nozzle can be subdivided in a manner similar to a jet-type inlet nozzle. Again, a high exit velocity would be difficult to achieve and formation of a large pool would be likely.

MINIMIZE LITHIUM WATER HAMMER EFFECT

Lithium that is in contact with target chamber structures at the time of the microexplosion will have shock waves developed in it by the neutrons and by the short-range radiations. This water hammer effect may cause structural damage depending on the intensity of the shock wave. The lithium fall design is intended to be at some distance from the first wall to minimize water hammer. However, at both the inlet and exit nozzles it is not possible to keep all the lithium from wall contact. Two conditions can occur. One is where the lithium adjacent to the structure has vapor as a nearby interface. The other is where the lithium is completely enclosed by the structure such as in a pipe or nozzle. The former will typically occur at the exit nozzle where it is difficult to avoid having a lithium pool adjacent to the chamber bottom. The latter may occur in the inlet nozzles and tend to be caused by neutrons since the short-range radiations are usually absorbed earlier. It is possible to reduce the harmful effects caused by lithium wall contact by having both a sufficient line-of-sight lithium thickness to attenuate the neutrons and having discontinuities in the lithium layers that protect the walls nozzles.

LITHIUM SPLASHING

The massive lithium flow rates (roughly 100 m^3/sec) will tend to create lithium splashing at the bottom of the chamber. The time of flight of droplets caused by splashing may be such that droplets are still in their trajectories when the next laser firing occurs. Such droplets have some chance of interfering with the laser beam on its way to the target. This problem can be eliminated by choosing relatively small chamber dimensions in combination with slow firing rates. Also, the hydraulic design of the chamber can be refined to minimize splashing, particularly in the region where the fall impacts the bottom of the chamber and the lithium velocities are at a maximum. Analysis and tests will be required to ensure relatively smooth flow from the fall into the exit nozzle. Splash suppression devices such as baffles or grids may be useful in reducing droplet formation.

PREVENTING PRESSURE BUILDUP

Following each microexplosion the pressure inside the annular fall, caused mainly by vaporizing lithium from the inner surface, will cause fall disassembly and loading to the chamber structures. One way to prevent pressure buildup is to vent the volume within the fall region to the space between the fall and the first wall or even outside the chamber. One approach is to replace the annular fall by an array of jet falls as previously discussed. The flow area of the vent paths must be large enough to prevent significant resistance to flow but sufficiently indirect to ensure that the first wall is protected from the neutrons. Venting not only increases the volume into which the lithium vapor can expand but promotes a stabilizing pressure on the outside of the fall. This also aids condensation since it provides a much greater surface and at a lower temperature than the inner surface of the fall. The inner surface of the fall sees the x-rays and other short-range radiations and is heated up to approximately the boiling point of lithium (1340°C). This surface temperature decays rather slowly because the vaporized lithium is momentarily well above the boiling point. On surfaces not exposed to short-range radiations the temperatures are initially 500°C so that lithium condensation can occur more readily. Venting decreases the effective lithium density and may require a greater line-of-sight lithium thickness, so that the required flow rate is expected to increase.

Another way to further promote lithium condensation is to provide sprays of lithium at various parts of the chamber. Such sprays could provide a large surface of relatively cool lithium upon which the lithium vapor could condense. Sprays would be particularly useful in the regions where the lithium vapor was vented.

Lithium sprays have another possible use in the target chamber. They can be used between the target and the fall for the purpose of absorbing the short-range radiations, thus reducing the magnitude of the shock wave generated in the liquid lithium.

NEUTRONIC STUDIES - INTRODUCTION

We now turn our attention from design considerations to the nuclear aspects of the target chamber. Neutronics studies have been made to determine how the system's nuclear performance varies as a function of the fall thickness. The TARTNP Monte Carlo neutronics code[3] has been used to determine several reactor system parameters including the tritium breeding ratio, the spatial energy deposition profile, the total energy deposition per DT fusion event, and the helium production and atomic displacement rates in the first structural wall. (While the results are presented as a function of lithium thickness, specific attention is given to the case of a 100 cm fall since this has been chosen for the point design for our reactor study. The point design has a thermonuclear yield of 2700 MJ at a repetition rate of 1.1 Hz and a first wall radius of 3.5 m).

SYSTEM MODEL

The one-dimensional, spherical geometry model used in this study is shown in Figure 1. A 14.1 MeV fusion neutron source is uniformily distributed throughout a DT fuel region that has a compressed density-radius product, ρR, of 3.0 gm/cm^2. The fuel region is surrounded by a pusher region that is compressed to $\rho\Delta R$ = 0.8 gm/cm^2. The neutron spectrum of this target with several different compressed configurations has been described previously.[4]

Surrounding the target is a 2 m region of lithium vapor, a variable thickness of liquid lithium representing the fall, another lithium vapor region between the fall and the first structural wall, and a graphite reflector outside the first wall. Table 1 gives a description of the zones.

NEUTRONICS MODEL

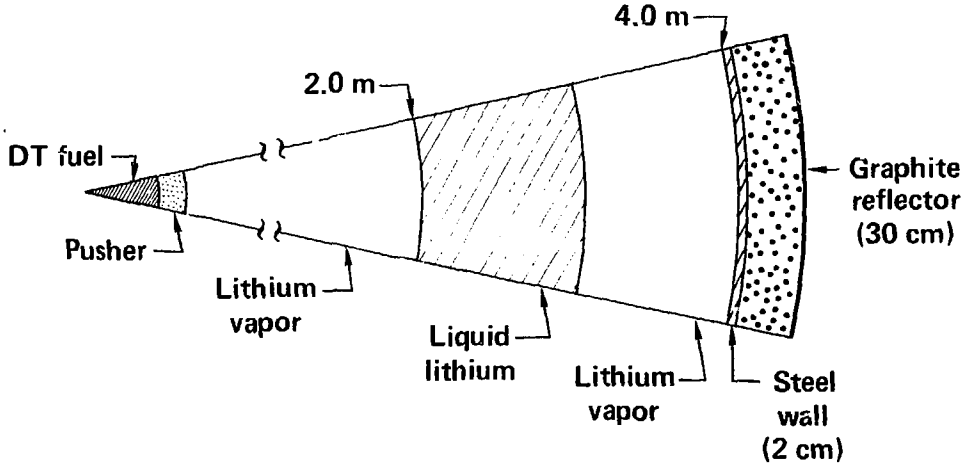

Figure 1

95-01-0478-1432

TABLE 1: Zone Description

Zone	Composition (a/o)	Density (gm/cm^3)	Inner Radius (cm)	Thickness (cm)
Fuel	D(0.5), T(0.5)		$\rho R = 3.0\ gm/cm^2$	
Pusher	D, T, C, O, W		$\rho R = 0.8\ gm/cm^2$	
Lithium: Vapor	$^6Li(0.0742)$, $^7Li(0.9258)$	1.4(-8)	0	200
Liquid		0.485	200	Variable,x
Vapor		1.4(-8)	200+x	200-x
Steel Wall*	Fe(0.994), Mo(0.006)	7.86	400	2
	Fe(0.885), Ni(0.115)	7.92		
Graphite Reflector	C(1.0)	1.70	402	30

* Ferritic steel, 2.25 w/o Cr, 1.0 w/o Mo with Cr replaced by Fe.
Austenitic steel, Type 316 SS, 18 w/o Cr, 12 w/o Ni with Cr replaced by Fe.

The neutron shield and pressure vessel wall have not been included in the calculational model. These components will have a negligible effect on the reactor parameters being investigated with the possible exception of the total energy deposition. It is likely that either B_4C isotopically enriched in ^{10}B or a region of liquid lithium will be used to absorb the neutron leakage from the graphite reflector. Both ^{10}B and ^{6}Li have high cross sections for exoergic absorption reactions with thermal neutrons and will thus result in a slight increase in the amount of energy deposited in the system. For example, even with a 100 cm thick fall, the neutron leakage per source neutron is $\sim$ 10%. If all these neutrons are absorbed in ^{6}Li or ^{10}B an additional 0.5 MeV or 0.3 MeV will be deposited in the system.

TRITIUM BREEDING

The tritium breeding performance is given in Table 2. For this reactor configuration a minimum of 40 cm of lithium is required to obtain a tritium breeding ratio greater than 1.0. For our current reference case of a 100 cm lithium fall the tritium breeding ratio is 1.6. Potentially, this excess tritium could be useful for fueling other DT fusion applications where tritium breeding is more difficult. If no market develops for the tritium a neutron poison could be added to the lithium stream to compete with the lithium for neutrons.

ENERGY DEPOSITION

The neutron induced energy deposition in MeV per DT reaction is shown in Figure 2. The curves show how the energy deposition in the different zones varies with the fall thickness. For a selected fall thickness a spatial energy deposition profile can be constructed from these curves. The curve labeled "total" is the sum of the lower three curves plus the energy leakage.

Note that on the average neutrons deposit 2.1 MeV or 15% of their original 14.1 MeV in the fuel target. This energy plus the 3.5 MeV alpha particle energy accounts for 32% of the target energy and is delivered in the form of x-rays and debris to the inner surface of the fall. Exoergic neutron reactions with blanket materials (primarily ^{6}Li) result in a net energy gain for the system. We define the blanket energy multiplication, M_B, as the ratio of the neutron induce energy deposition outside the target to the neutron energy leaving the target (i.e., 68% of 17.6 MeV in this case). It is higher than the system energy multiplication, M_S, which is defined as the total energy deposited in the system (neutron plus alpha) divided by 17.6 MeV.

TABLE 2: Tritium Breeding Performance

Fall Thickness (cm)	T_6	T_7	T_{total}
40	.52	.49	1.01
60	.71	.59	1.30
80	.84	.65	1.49
100	.94	.67	1.61
120	1.01	.68	1.69

$T_6 = {}^6Li(n,\alpha)T$
$T_7 = {}^7Li(n,n'\alpha)T$

NEUTRON PLUS NEUTRON INDUCED PHOTON ENERGY DEPOSITION

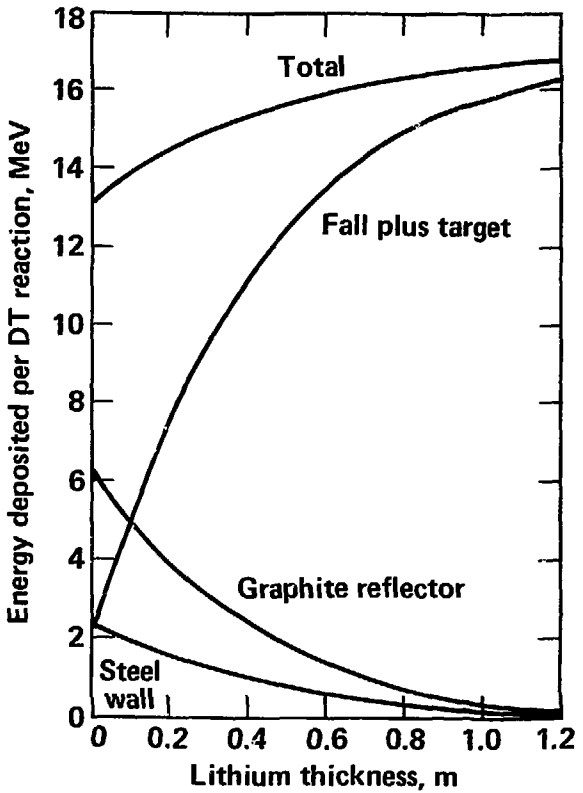

95-01-0478-1471

Figure 2

Table 3 gives a more detailed breakout for the case of a 100 cm thick lithium region and shows the energy deposition from neutrons and neutron induced photons. The system energy multiplication is 1.14. If the neutron leakage times 4.8 MeV is added to the total as previously discussed, the total energy deposition is 20.5 MeV, M_B equals 1.24 and M_S increases to 1.16.

For the present configuration of the reactor system it is necessary to deposit as much of the system energy as possible in the lithium region. For our reference case of a 100 cm fall, greater than 96% of the total system energy is deposited directly in the lithium.

RADIATION DAMAGE

Radiation damage to the first structural wall is being evaluated in terms of two parameters; the helium production rate and the atomic displacement rate. Both rates are time integrated and do not represent the instantaneous rate at the time of the fusion event.

Both rates are expressed per unit equivalent neutron wall loading to facilitate comparison to other fusion concepts. The equivalent neutron wall loading is defined as

$$\phi_n = .8(P_{TN})/4\pi R^2$$

where P_{TN} = Thermonuclear Power (yield x rep. rate), MW; and R = First wall radius, m. For our reference case of 2970 MW and the first wall at 3.5 m, $\phi_n = 15.4$ MW/m^2.

HELIUM PRODUCTION

The helium production rate is determined directly from the reaction edits of the TARTNP code. The helium production rate per unit neutron-first-wall-loading is calculated from

$$R = 10^6 \text{ G/ENT}$$

where R = production rate, appm per MW-yr/m^2

G = helium producing reactions per source neutron, He/n

E = energy per source neutron, MW-yr/n

N = atom density of steel, atoms/m^3

T = wall thickness, m

TABLE 3: Energy Deposition - 100 cm Thick Fall

	MeV per DT Reaction		
Zone	Neutron	Photon	Total
Fuel	1.91	4.8(-4)	1.91
Pusher	0.23	1.0(-3)	0.23
Lithium Fall	13.34	0.35	13.69
Steel Wall	0.01	0.24	0.25
Graphite Reflector	0.19	0.19	0.38
Leakage	.05	.05	.10
Total neutron, gamma	15.73	0.83	16.56
Total alpha			3.5
TOTAL			20.06*

* Capture of leakage neutrons in ^{6}Li gives E_{TOTAL} = 20.5 MeV.

For the present problem, E is a constant and equal to 7.163×10^{-26} MW-yr/n; N varies slightly from steel to steel but is about 8.5×10^{28} atoms/m^3; T will be determined by the design of the first wall but has been assumed to be 2 cm in calculations to date. The number of reactions per source neutron, G, is directly related to the reaction cross sections.

Figure 3 compares the helium production cross sections (n,α) plus $(n,n'\alpha)$ from the Livermore Evaluate Nuclear Data Library, ENDL and the Brookhaven Evaluate Nuclear Data File, ENDF/B-IV. Most notable is the large discrepancy in the cross sections for iron. The ENDF value is higher than the ENDL value; at 15 MeV it is only 25% greater but the difference increases with decreasing neutron energy to a factor of 7 higher at 9 MeV. This discrepancy is due to the lack of experimental measurements and the fact that the systematics for calculating cross sections are not all that well developed. Since the products of (n,α) and $(n,n'\alpha)$ reactions with ^{56}Fe (92% of natural iron) are the stable isotopes ^{53}Cr and ^{52}Cr, these cross sections cannot be measured by conventional activation techniques. No measurements of helium production cross sections have been made on natural iron and only one measurement has been made for ^{56}Fe.[5] This one point measurement was at 14.6 MeV.[6]

To determine what effect this cross section discrepancy would have on the helium production rate, the case of a 100 cm thick fall and 2 cm iron wall was run with the two different libraries. The result was that the ENDF/B-IV library gave a helium production rate 2.6 times greater than the ENDL library.

The cross sections for nickel agree quite well, reflecting the fact that the (n,α) cross section for ^{58}Ni (68% of natural Ni) can be evaluated from activation data. The ENDL library does not contain a cross section for chromium due to the lack of experimental data. The ENDF cross section for chromium is included in Figure 3 and falls between the two library's cross sections for iron.

Since ENDL does not include a helium production cross section for Cr, in this study the Cr content of the first structural wall has been replaced by Fe. The assumption implied here is that Cr has alpha producing cross sections similar to those for Fe. Our prime candidate for a structural material, the ferritic alloy 2.25 Cr-1.0 Mo, has such a low Cr content that the substitution of Fe for Cr should introduce a negligible perturbation.

COMPARISON OF HELIUM PRODUCTION CROSS SECTIONS

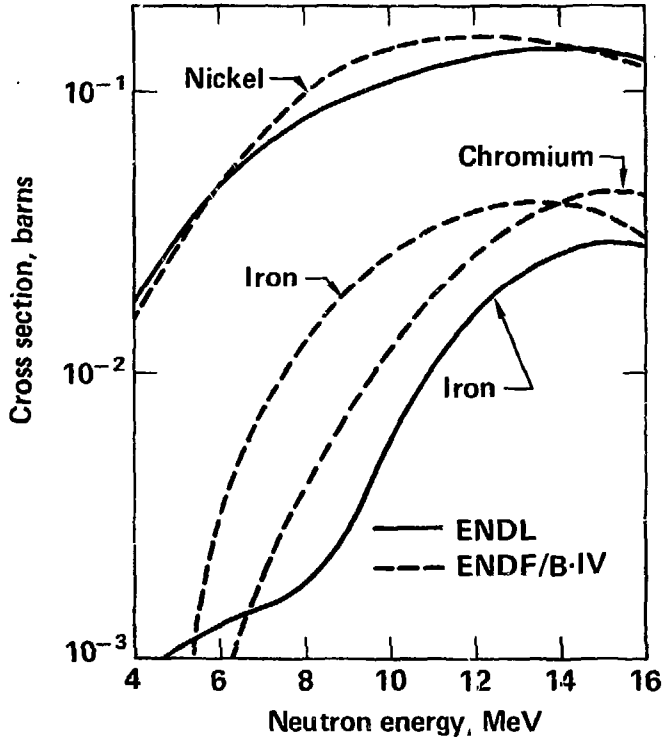

95-01-0478-1425

Figure 3

For comparison, the helium production rate in Type 316 stainless steel has also been examined. Here, 88% Fe and 12% Ni was used instead of using 70% Fe, 18% Cr and 12% Ni. The resulting helium production cross section at 15 MeV is $\sim$ 42 mb. A recent measurement of 316-SS at Livermore's RTNS produced a value of 48 $\pm$ 7 mb at 15 MeV.[7] Thus the value used in these neutronics calculations is within the uncertainty range, but on the low end, of the measured experimental value.

The reduction in the helium production rate realized by protecting the first wall by a region of lithium is illustrated in Figure 4. Shown is the production rate in appm-He per year per (MW/m^2) of equivalent neutron wall loading. Note that the nickel content of Type 316 stainless steel results in a helium production rate that is about a factor of two greater than the ferritic steel.

The production rate in the ferritic wall protected by 100 cm of lithium is 0.6 appm per ($MW\text{-}yr/m^2$) or 9.3 appm per year for our reference case at 15.4 MW/m^2. Over a 30 year operating life at 70% capacity factor, the accumulated helium concentration is less than 200 appm. For the stainless steel wall the value is 420 appm helium.

Atomics International has studied the effects of helium on the tensile properties of alloys by injecting helium into miniature tensile specimens by alpha-particle irradiation. They have found that austenitic samples with low helium concentrations (40 appm) lose ductility more rapidly with increasing temperature than do ferritic steels with the same helium content.[8,9] Twenty percent cold-worked Type 316 stainless steel irradiated at ORNL and tensile tested at 575 C retained a total and uniform elongation of 1.5% while containing 2030 appm helium.[10] If the superior ductility retention of a ferritic steel can be extrapolated to a high helium regime then we can expect ferritic steels to retain at least a couple percent elongation at 500 C with greater than 2000 appm helium. (Current design minimums for uniform elongation in the LMFBR program range from 0.2% to 0.5%). Helium production, therefore, does not appear to be a limiting factor for our design.

REDUCTION OF HELIUM PRODUCTION RATE BY LITHIUM FALL

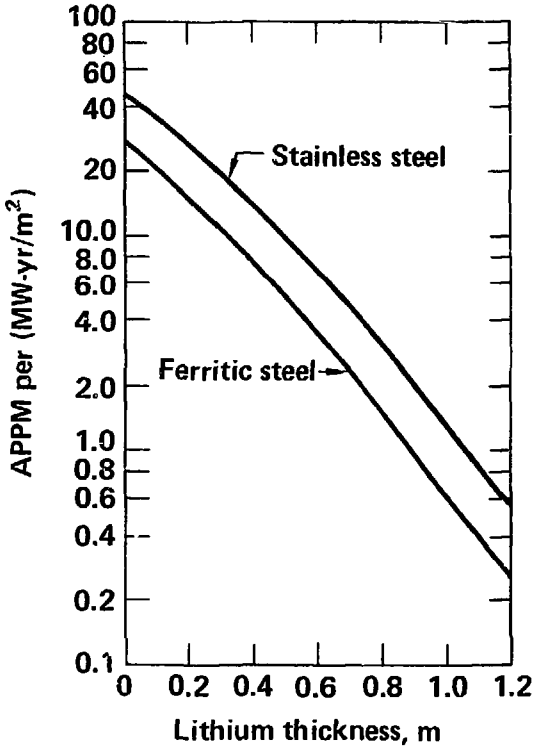

95-01-0478-1434

Figure 4

DISPLACEMENT DAMAGE

Displacement damage rates were calculated using the modified cross sections calculated by Doran and Graves.[11] These cross sections are somewhat higher than an earlier set[12,13] used in similar studies.[14,15] The cross sections for iron and 18-10 stainless steel (similar to Type 316) are shown in Fig. 5 collapsed to the 50 energy group structure of TARTNP. They are essentially the same with the iron cross section being slightly lower than that for SS. The recommended value of 40 eV was used for the effective displacement energy. For neutron energies less than 10^{-4} MeV, the displacement cross section varies as $E^{-1/2}$ from values of 17b and 20b for iron and SS respectively at 0.025 eV.[12]

The effectiveness of the lithium fall in reducing the displacement damage rate in iron is shown in Figure 6. The displacement rate per unit equivalent neutron wall loading is calculated from

$$R = \sum_i \sigma_i F_i/(E/A)$$

where R = displacement rate, dpa per (MW-yr/m^2)

σ_i = energy dependent displacement cross section, dpa per n/cm^2

F_i = energy dependent neutron fluence, n/cm^2 per source neutron

E/A = equivalent neutron wall loading, E=7.163 x 10^{-26} MW-yr per source neutron, A = wall area = 4 R^2 for this study.

For 100 cm of protection the dpa rate is reduced to $\sim$.5 dpa per (MW-Yr/m^2). For our reference case at σ_n = 15.4 MW/m^2, the total accumulated displacement damage after 21 full power years is 162 dpa. The result for the 18-10 SS is only about 10 dpa higher.

Radiation induced swelling is generally assumed to be a linear function of dpa after some incubation dpa. Iron irradiation experiments of ferritic alloys indicate that they are more swelling resistant than Type 316 stainless steel. Using the correlations given in reference 16, the high Cr ferritic alloys EM12(9% Cr) and HT9(12% Cr) would show 1.6% and 3.4% swelling after 162 dpa at their peak swelling temperatures of 550°C and 500°C respectively. However, neutron irradiation temperatures generally correlate to an ion irradiation temperature about 100°C higher. Therefore, the expectation is that little swelling will occur in either of these alloys under our system

DISPLACEMENT CROSS SECTIONS

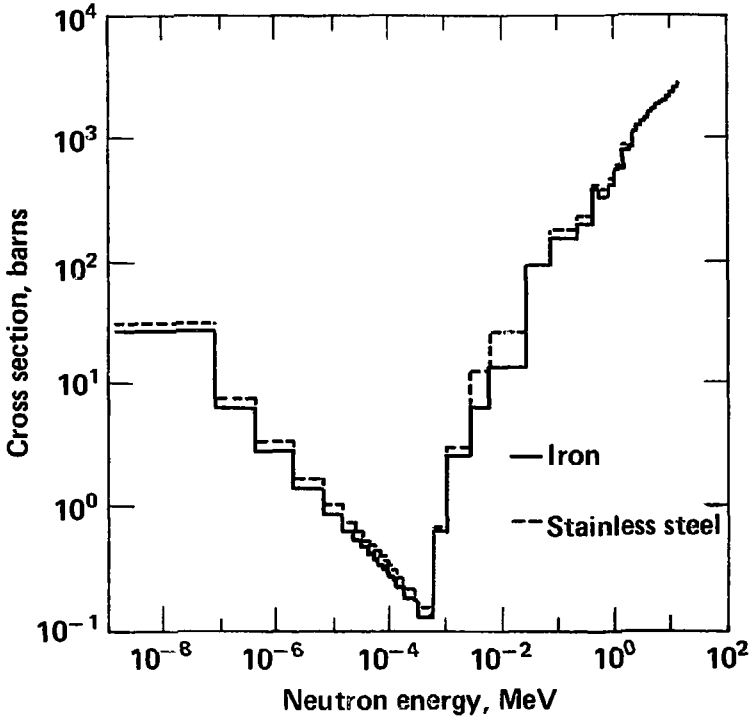

95-01-0478-1427

Figure 5

REDUCTION OF DISPLACEMENT DAMAGE RATE BY LITHIUM FALL

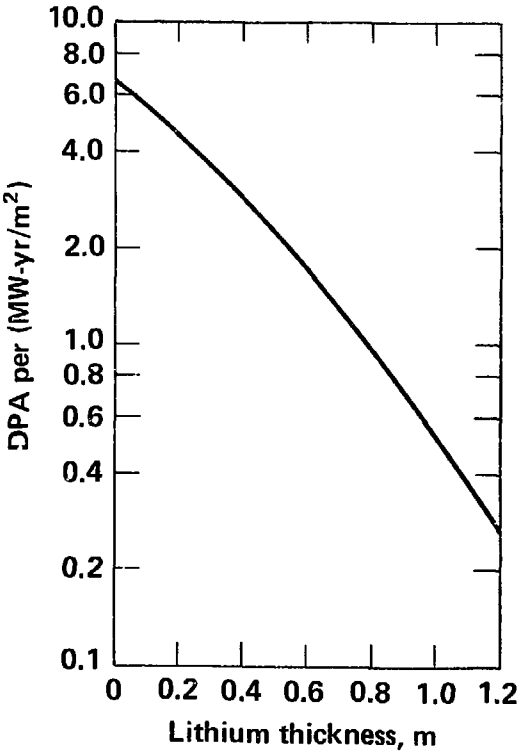

95-01-0478-1433

Figure 6

conditions of neutron irradiation at 500 C because little swelling occurs at 600°C during ion irradiation. There is also evidence that, to a point, swelling increases with increasing Cr content and, thus, the 2.25 Cr-1 Mo alloy considered for our design would exhibit even less swelling under the same conditions. (2.25 Cr-1 Mo showed only 0.8% swelling after 115 dpa at 550 C).[16]

Even 20% cold-worked Type 316 stainless steel, which is more swelling resistant than annealed SS, shows a swelling rate that is 4 to 6 times greater than ferritic alloys HT-9 and EM-12. From the correlation in Ref. 10, 20% cold-worked 316-SS would have 10.5% swelling after the 172 dpa expected after 30 years in our reactor system. A maximum of 10% swelling has previously been suggested as an end of life damage limit for Tokamaks.[15] Thus, even stainless steel could be used in our system using these radiation damage limitations.

CONCLUSIONS

In terms of nuclear performance the most unique feature of the fluid wall designs is that the energy absorbing "blanket" region (lithium fall) is actually inside the first structure wall. By requiring that 95% of the system energy is deposited in the lithium within the vacuum chamber, radiation damage is essentially eliminated as a design constraint. We have also found that such designs result in high blanket energy multiplication and high tritium breeding ratios. Ferritic steels, which show greater resistance to lithium corrosion, also appear to be less susceptible to radiation damage.

Design considerations relating to the configuration of the lithium fall, hydraulic effects within the chamber, pressure suppression, nozzle design and laser beam entry have also been discussed. Design options have been identified that mitigate the problems associated with the annular fall design. Such studies are resulting in the continual evolution and improvement of the fluid wall reactor concept for laser fusion.

REFERENCES

1. J. Hovingh, J.A. Blink, L. Glenn, "The Response of a Lithium Fall to an Inertial Confinement Fusion Microexplosion," Proceedings, 3rd Topical - Technology of Controlled Nuclear Fusion, May 9-11, 1978, Santa Fe, NM.

2. J.A. Maniscalco, et.al., "A Laser Fusion Power Plant Based on a Fluid Wall Reactor Concept," Proceedings, 3rd Topical - Technology of Controlled Nuclear Fusion, May 9-11, 1978, Santa Fe, NM.

3. E.F. Plechaty, J.R. Kimlinger, "TARTNP: A Coupled Neutronic-Photon Monte Carlo Transport Code," Report UCRL-50400, Vol.14, 1976.

4. J.A. Blink, P.E. Walker, H.W. Meldner, "Energy Partition and Neutron Spectra From Laser Fusion Reactor Targets," Transactions of 1977 ANS Winter Meeting, p.70.

5. M.H. Macgregor, et.al., "Neutron-Induced Interactions: Index of Experimental Data," UCRL-50400, Vol.3, Rev. 2, 1976.

6. C. Spera, J.M. Robson, Nuclear Phys. 127, 81, 1969.

7. R.C. Haight, S.M. Grimes, J.D. Anderson, "Hydrogen and Helium Production Cross Sections for 15 MeV Neutrons on Type 316 and 304 Stainless Steel," Nuc. Sci. & Eng., 63, 2, June 1977.

8. D. Kramer, et al., Trans. Met. Soc. AIME, 245, 1909, 1969.

9. D. Kramer, et al., J. Iron Steel Inst., 207, 1141, 1969.

10. E.E. Bloom, et al., "Temperature and Fluence Limits for a Type 316 Stainless Steel CTR First Wall," Nuc. Tech. 31, Oct. 1976.

11. D.G. Doran, N.J. Graves, "Neutron Displacement Damage Cross Sections for Structural Metals," Irradiation Effects on the Microstructure and Properties of Metals, ASTM STP 611, 1976, pp.463-482.

12. D.G. Doran, Nucl. Sci. Eng. 49, 130, 1972.

13. D.G. Doran, Nucl. Sci. Eng. 52, 398, 1973.

14. G.L. Kulcincki, et al., "Protection of CTR Metallic First Walls by Neutron Spectral Shifting," Univ. of Wisc. Report, UWFDM-127, 1975.

15. H.I. Avci, G.L. Kulcinski, "The Effect of a Liquid ISSEC on Radiation Damage Parameters in Laser Fusion Reactor First Walls." Univ. of Wisc. Report, UWFDM-205, 1977.

16. F.A. Smidt, Jr., "Swelling Behavior of Commercial Ferritic Alloys, EM-12 and HT-9, as Assessed by Heavy Ion Bombardment," Irradiation Effects on the Microstructure and Properties of Metals, ASTM STP 611, 1976, pp.227-241.

17. G.L. Kulcinski, et al., "Radiation Damage Limitations in the Design of the Wisconsin Tokamak Fusion Reactor," Nuc. Tech., 22, 20, 1974.